Fifth International Symposium on Marine Propulsion
smp'17, Espoo, Finland, June 2017

Cavitation erosion fracture mechanisms and their detection in ship operation

Ioannis Armakolas, John Carlton, Miodrag Vidakovic, Tong Sun and Kenneth T. V. Grattan

School of Mathematics, Computer Science & Engineering, City University of London, London, United Kingdom

ABSTRACT

This paper explores the phenomenon of cavitation erosion in relation to common shipbuilding materials such as grade DH36 steel, cupronickel and stainless steel. Experimental findings regarding the resulting mass loss as well as the underlying fracture mechanisms of erosion on those materials due to ultrasonically induced cavitation are initially presented. In addition, acoustic emissions (AE) relating to ultrasonically induced cavitation erosion are explored and measured using both piezoelectric and fibre Bragg grating (FBG) based sensing systems, for a range of test rig configurations leading to cavitation of varying severity, ranging from non-erosive to highly erosive. A method through which acoustic emissions are translated into acoustic power and stress units is then presented along with the main findings in terms of correlation with cavitation erosion severity. Promising results lead to the application of the method on a reduced–scale rudder model. Apart from cavitation erosion severity acoustic emission measurements, a cavitation source location method based on the principle of triangulation is also explored and presented. Results indicate that acoustic emissions can potentially be used as means of cavitation erosion monitoring.

Keywords

Cavitation erosion, Rudder, Structural health monitoring, Acoustic emissions, Non-destructive testing (NDT).

1 INTRODUCTION

Ships play a dominant role in the global trade, as significant percentage of Earth's surface is covered by water and they carry about 90% of goods. Some of their mechanical components however, such as rudders and propellers, are often exposed to harsh operational environments and as such can be subject to significant deterioration. Corrosion and erosion are mainly responsible for this deterioration, the former caused by the electrochemical interaction between the mechanical components and the seawater and the latter by phenomena such as cavitation (Carlton 2012).

Cavitation is a general fluid dynamics phenomenon and can be defined as the rapid formation, growth and subsequent collapse of very small bubbles or cavities within a liquid due to large pressure or velocity variations which are common in mechanical components of ships such as rudders and propellers. Cavitation was first mentioned by Euler (1756) and had not been studied until the middle of the 19th century (Besant 1859, Reynolds 1873). In the beginning of the 20th century Lord Rayleigh (1917) undertook a significant effort in his analysis of bubble collapse dynamics and suggested a basic cavitation mechanism, followed by Parsons & Cook (1919).

Recent studies, conducted with the aid of high speed photography, revealed high pressure waves emitted from collapsing bubbles (Philipp & Lauterborn 1998, Lindau & Lauterborn 2003). Some researchers suggested that for specific geometries the collapse energy of a large cavity can be oriented into a small region of the adjacent solid surface and induce significant erosion as a result (Bark et al 2004). Others proposed that macro cavities can be converted into collapsing clouds of micro bubbles emitting erosive shock waves (Fortes-Patella et al 2004). Nevertheless, the ultimate nature of the cavitation erosion mechanism is still debatable and phenomena such as bubble collapse and rebound, micro jet formation, clouds of collapsing micro bubbles and cavitation vortices are believed to be the dominant candidates (Franc & Michel 2004).

With regards to the effects of cavitation in terms of mass loss it has been suggested that erosion mainly progresses in four distinct phases, namely the incubation, acceleration, steady state and deceleration phases (Karimi & Martin 1986). This observation is only valid from a qualitative point of view, however, whereas the quantitative aspects of the rate of mass loss cannot be predicted as accurately and should be calculated individually for each material.

This research, rather than exploring the possible erosion mechanisms from a hydrodynamic point of view, focused on the immediate effects of cavitation erosion on common shipbuilding materials. As such specimens were exposed to ultrasonically induced cavitation in water and a series of qualitative and quantitative procedures took place including mass loss measurements and optical observations through a scanning electron microscope SEM). In addition, the possibility of utilizing acoustic emissions as means of cavitation erosion monitoring in terms of location and severity was also explored.

2 EXPERIMENTAL TEST RIG

Cavitation was induced by ultrasonic means and as such an appropriate test rig was built to accommodate both the ultrasonic transducer and the examined specimens. The test rig is presented in Figure 1.

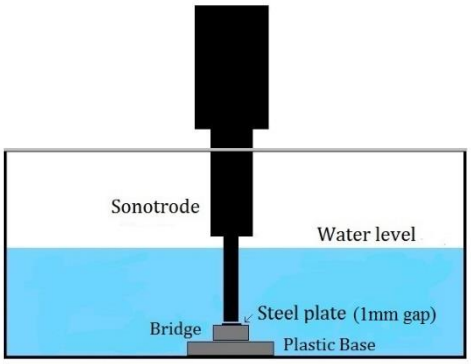

Figure 1: Illustration of the experimental test rig showing the sonotrode, the main tank and a mounted steel sample.

The ultrasonic transducer that was used was the Hielscher UIP 1000hD with a maximum power output of 1000W, adjustable in 50W steps. The sonotrode (probe head) of the transducer oscillates at a frequency of 19.5 kHz thus it induces cavitation through fluctuation of water pressure, locally. Specimens, in the form of 50 x 50 x 5 mm rectangular plates, were mounted firmly on a plastic bridge - base, positioned just below the oscillating sonotrode head, at a predetermined distance. In the case of long lasting cavitation exposure and due to heat accumulation from the operation of the sonotrode, water was recirculated through a larger tank to keep the temperature steady.

3 MASS LOSS MEASUREMENTS

Specimens made from grade DH36 steel, stainless steel 254 and cupronickel 70-30 were initially exposed to ultrasonically induced cavitation for a period of five (5) hours, under identical experimental conditions. Mass loss measurements were conducted every thirty (30) minutes and as such the progression of their mass loss, through the five (5) hours exposure period, of each of the examined metals due to erosion, was calculated. Comparative results are presented in Figure 2.

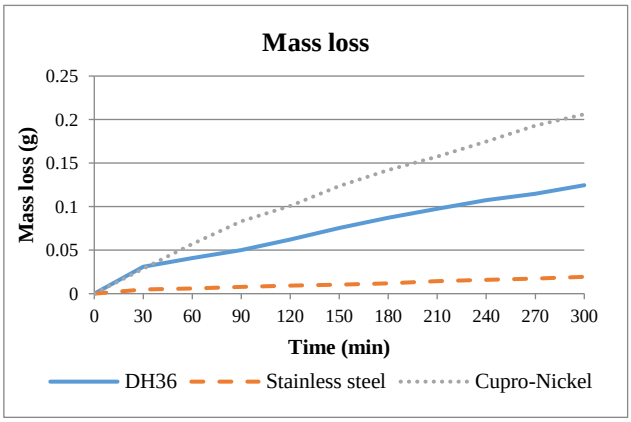

Figure 2: Mass loss comparison between three different metals.

A gradual increase of mass loss can be observed for all metals. The slope of the mass loss lines, however, varies significantly with regards to the examined material, thus indicating dissimilar rates of mass loss. Under this context it appears that, in general, cupronickel 70-30 exhibited higher rates of mass loss followed by grade DH36 steel and stainless steel.

From a quantitative point of view, stainless steel 254 exhibited the best behaviour in terms of measurable cavitation erosion resistance, with a total mass loss of the order of 0.02g, followed by grade DH36 steel with 0.13g and cupronickel 70-30 with 0.21g. The progression of mass loss for the latter is identical for the first thirty (30) minutes of exposure, however, the total difference at the end of procedure is 0.08g in favour of grade DH36 steel. This indicates an identical behaviour during the first thirty (30) min for cupronickel 70-30 and grade DH36 steel whereas the subsequent difference with regards to the slope of their mass loss lines, for the rest of the procedure, indicates a more resistant material in the name of grade DH36 steel, possible due to work hardening effects.

All results, as well as the specific experimental conditions, were highly reproducible and as such it was proven that the method can be used as a baseline for comparative measurements between different materials with regards to ultrasonically induced cavitation erosion.

4 FRACTOGRAPHY

Following the five (5) hours cavitation exposure, specimens were also examined in relation to the appearance of their surface, in order for particular characteristics related to cavitation erosion to be identified. Specimens were initially examined under the lens of an optical microscope, the underlying fracture mechanisms however were not revealed until they were examined by means of a Scanning Electron Microscope (SEM) with much higher magnification and focus capabilities. SEM images are presented in Figure 3.

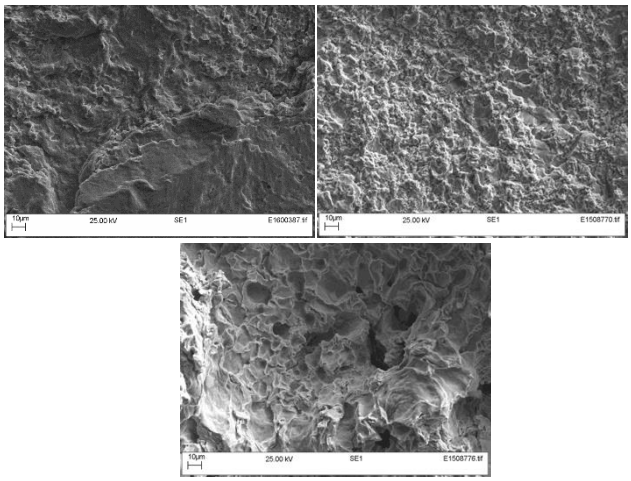

Figure 3: SEM images of the three metals after five (5) hours of ultrasonically induced cavitation exposure. Top left – Grade DH36 steel, Top Right – Stainless steel 254, Bottom – Cupronickel 70-30.

The appearance of the eroded surface of grade DH36 steel is characterized by ridges and smooth bumps, which can be regarded as typical features of transgranular brittle fracture (fracture propagation through the grains of the metal). Elements of intergranular brittle fracture (fracture propagation through the grain boundaries of the metal) can also be seen in the form of small well – defined facets in addition to a considerable amount of ductile dimples possibly related to plastic deformation.

Similarly, the eroded surface of stainless steel 254 is characterized by a combination of mainly transgranular brittle fracture and to a lesser extent intergranular brittle fracture and plastic deformation. The latter are again characterized by small well–defined facets and ductile dimples, respectively, whereas characteristics of the dominant transgranular brittle fracture can be identified in the form of ridges and smooth bumps.

Finally, the appearance of the eroded surface of cupronickel 70-30 is characterized by ductile dimples of all sizes, hence plastic deformation appears to be the dominant fracture mechanism in that instance. Signs of transgranular brittle fracture cannot be identified although an amount of intergranular fracture could be apparent at some areas resembling the undamaged grain structure of the material.

The combination of mass loss data and SEM fractography indicates a connection between those factors. More specifically it appears that, plastic deformation is accompanied by an increased amount of mass loss whereas the opposite behaviour is characterized by signs of brittle fracture, possibly due to the appearance of work hardening effects. This is particularly apparent in the case of cupronickel 70-30 which exhibited the highest mass loss between the examined materials and its eroded surface is dominated by signs of plastic deformation. On the other hand, grade DH36 steel, experienced a lower amount of mass loss and its surface is mostly characterized by signs of brittle fracture and to a lesser extent plastic deformation. Stainless steel exhibited a minimal amount of mass loss compared to the other two metals and its surface is dominated by signs of brittle fracture whereas signs of plastic deformation are hardly identifiable.

Results indicate that the type of fracture (brittle or ductile) experienced by the materials, due to ultrasonically induced cavitation, could possibly be explained by their corresponding behaviour in terms of the measured mass loss. The underlying fracture mechanisms however, such as the type of brittle fracture experienced by the material (transgranular or intergranular) cannot be predicted as accurately as they are possibly related to its unique mechanical and chemical properties.

5 THE USE OF ACOUSTIC EMISSIONS

A brief summary of the history behind the use of acoustic emissions as means of a monitoring tool, as well as the working principles of the acoustic sensors that were used, are initially presented in this section. Afterwards, the application of acoustic emission measurements for cavitation erosion evaluation purposes, held in small specimens, are presented along with the relevant findings. Finally, an investigation regarding the use of acoustic emissions as means of cavitation erosion monitoring, both in terms of location and intensity, on a reduced-scale rudder model is presented.

5.1 Acoustic emissions

Acoustic emissions can be defined as the elastic stress waves produced when metals absorb and release strain energy and stress. The mechanisms by which a metal undergoes internal transformation and releases high frequency elastic stress waves or acoustic emissions, are the basis of fracture mechanics. In particular, plastic deformation as well as crack growth and propagation are the primary sources of acoustic emissions in metals (Rogers 2001).

The first official report of acoustic emissions generated from a metal under stress was made by Portevin & Le Chatelier (1923) and has not been further investigated until almost 30 years later (Kaiser 1953, Schofield 1958). One of the most important findings regarding acoustic emissions is that their amplitude is directly related to the severity of the internal fracture event, therefore they attracted a lot of interest in the following years by researchers who started considering the use of acoustic emissions as means of a structural monitoring system (Pollock 1968, Dunegan 1969, Votava & Jax 1979).

Following successful application for over four decades, acoustic emissions are still used for non–destructive monitoring purposes in a variety of structures such as bridges and historical buildings (Carpinteri et al 2007). The non – destructive nature of the method as well as the ability to monitor structures remotely and accurately have contributed significantly to a continuous interest from the industry (Tan et al 2009).

Cavitation related erosion can be regarded as one of those cases where an exposed metal undergoes stress loading and as a result several internal fracture events release that stress in the form of acoustic emissions. As such it was decided to investigate the resulting acoustic emissions due to ultrasonically induced cavitation erosion and explore whether they can be used for monitoring purposes or not.

5.2 Piezoelectric and Fibre Bragg grating acoustic sensors

Acoustic emissions are measured by means of acoustic sensors. In this study, two types of acoustic sensors were used, namely piezoelectric and fibre Bragg grating sensors.

The operation of piezoelectric sensors is based on the principle of piezoelectricity, which is the ability of some materials to produce an electrical charge in response to an applied mechanical stress (Gautschi 2002). Piezoelectric acoustic sensors can be used either actively, where the sensors generate ultrasonic signals (Giurgiutiu 2003), or passively, where the sensors essentially measure ultrasonic signals (acoustic emissions) generated by the examined structure itself, due to internal fracture events (Mal et al 2003). It should be noted that for the purpose of this study piezoelectric sensors were used passively, always in

conjunction with essential supportive equipment such as preamplifiers as well as signal attenuators and detectors.

Fibre Bragg grating (FBG) acoustic sensors on the other hand are essentially optical sensors that reflect a specific wavelength of light and transmit all others, thus any induced mechanical strain results into a reflected – wavelength shift that can be measured (Othonos & Kalli 1999). They have shown a great potential for applications in highly demanding and harsh environments such as in biomechanics and engineering due to their immunity to electromagnetic interference (EMI), small size, cost and chemical inertness (Grattan & Sun 2000, Mihailov 2012).

The acoustic emission monitoring system that was built for this study is illustrated in Figure 4, showing both the piezoelectric and fibre Bragg grating acoustic sensors as they were mounted on a steel plate specimen in conjunction with all the relevant supportive equipment.

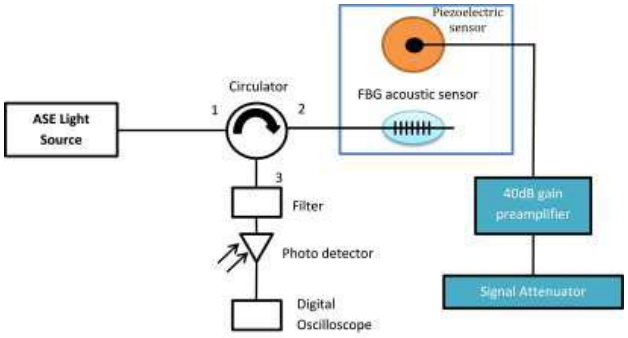

Figure 4: Acoustic emission monitoring system including both piezoelectric and FBG acoustic sensors mounted on a steel plate.

With regards to the piezoelectric sensor, signal pre–amplification as well as noise attenuation modules are included to optimize the output of the sensor. The fibre Bragg grating (FBG) sensor on the other hand requires the use of an appropriate light source in conjunction with a photodiode. Signals originating from both types of sensors were captured by means of a high frequency oscilloscope and were further processed through a computer.

5.3 Acoustic emission measurements on small plates

Preliminary measurements were conducted using both types of acoustic sensors, piezoelectric and fibre Bragg gratings. The main scope of those measurements was to explore whether the acoustic sensors are capable of identifying cavitation erosion related resonances or not.

Towards that direction, a small steel plate was exposed to ultrasonically induced cavitation, similar to the initial mass loss measurements, whereas piezoelectric and fibre Bragg grating acoustic sensors were attached on the opposite, to the exposed surface, side. Time domain acoustic emission signals were captured through a digital oscilloscope and were further processed by means of a Fast Fourier transform (FFT).

The frequency response obtained for both types of acoustic sensors by means of a Fast Fourier transform (FFT) is presented in Figure 5.

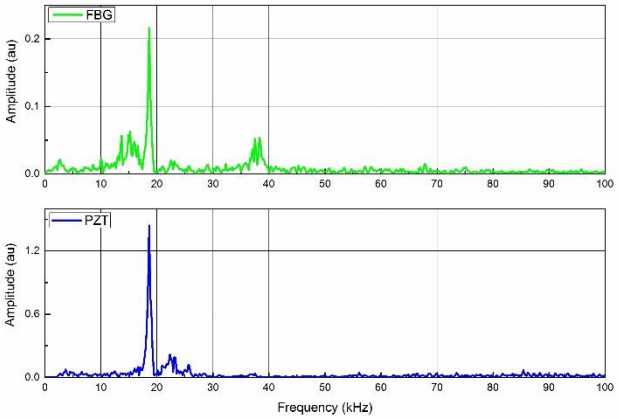

Figure 5: Frequency response spectra through the 0-100 kHz range. Top – FBG, Bottom – piezoelectric.

A common frequency component is apparent on both frequency domain spectra. This is the 19.5 kHz resonance which matches the operating frequency of the ultrasonic transducer and it is directly related to the internal response of the steel plate in the form of acoustic emissions, due to the ultrasonically induced cavitation loading,

Following successful detection of ultrasonically induced cavitation activity on a steel plate, in the form of the dominant frequency component, it was decided to create a methodology through which acoustic emission signals, which are basically electrical signals, would be translated into stress loading values. This methodology was based on the use of piezoelectric acoustic sensors, due to their demonstrated linear behaviour, in the sense that the amount of electrical charge generated is strictly proportional to the applied force.

An initial calibration using a known force, was conducted, in order for a baseline to be established, with regard to the conversion coefficient between the produced electrical charge and the induced stress. Calibration was conducted by means of a Hsu – Nielsen (HN) source, which is essentially the fracture of a 0.5mm diameter 2H graphite lead on the surface of the examined material. A single fracture event equals to one (1) HN unit corresponding to a predetermined value of stress and a specific acoustic emission signal in terms of voltage. Following initial calibration, the relation between induced stress and voltage is given by Equation (1).

$$\sigma = kV \qquad (1)$$

where σ = induced stress in MPa, V = the peak voltage of the acquired acoustic emission signal and k = the coefficient which is unique and characteristic of the specific piezoelectric sensor as well as of the examined material and defines the relation between the induced stress and the generated electrical signal.

Once the relationship between induced stress and acquired acoustic emissions in voltages was established for each one of the examined materials it was decided to conduct a series of acoustic emission measurements and explore the relation between the obtained stresses and the intensity of cavitation in terms of erosion–mass loss. As such four

different test rig configurations were examined for each one of the examined materials, leading to cavitation of varying intensity, ranging from 'non-erosive' to 'highly erosive' always in terms of the corresponding mass loss.

Acoustic emission signals for each one of the aforementioned cavitation conditions and materials were then translated into stresses by means of Equation (1) and were plotted onto frequency distribution graphs, as cavitation erosion is essentially represented through multiple fracture events. The stress distributions of grade DH36 steel, stainless steel and cupronickel are presented in Figure 6.

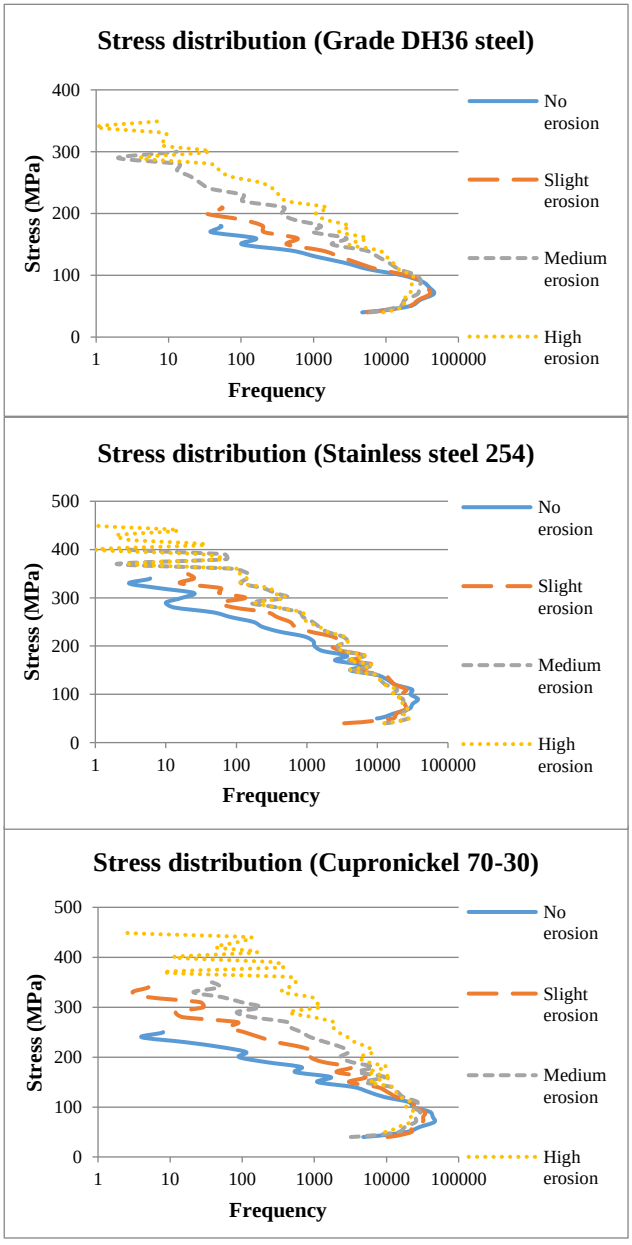

Figure 6: Stress distributions obtained from acoustic emission signals. Top – Grade DH36 steel, Middle – Stainless steel 254, Bottom – Cupronickel 70-30.

Solid lines represent the 'no-erosion' cavitation conditions for which no mass loss could be measured. Those conditions were different for each one of the materials and this is represented by the dissimilar stress values obtained. Stainless steel for instance, which was more resistant in terms of mass loss, could withstand cavitation of higher intensity compared to the other two metals and as a result, its 'non-erosive' condition corresponds to stresses of the order of 320 MPa. The 'non-erosive' cavitation conditions of Cupronickel and Grade DH36 steel on the other hand were identical and are represented by stresses of the order of 220 MPa and 180 MPa, respectively. Assuming similar cavitation conditions for the latter, this difference could be attributed to their internal structure.

With regards to its mechanical properties, results for grade DH36 steel indicate that for the 'non-erosive' conditions stresses (180 MPa) are well below the yield strength (350 MPa) of the material and below its endurance limit (245 MPa). The next 'slightly-erosive' configuration is represented by stresses of the order of 210 MPa, slightly below its endurance limit (245 MPa). This corresponds to a minor measurable mass loss. The other, more intense, settings are either well above the endurance limit (245 MPa) or comparable to its yield strength (350 MPa) of the material and as such the increased amount of measured mass loss is well justified.

Similar conclusions apply for stainless steel. Considering that its yield strength is 415 MPa and its endurance Limit is 345 MPa, the obtained stress values regarding the 'non-erosive' (320 MPa) and the 'slightly-erosive' (350 MPa) conditions are again sensible. As for the other two, more intense, conditions the obtained stress values are comparable or above the yield strength of the material and this is represented by an even higher amount of measured mass loss.

Finally, the obtained stress values for cupronickel, which are 220 MPa for the 'non-erosive' and 310 MPa for the 'slightly-erosive' condition are well above its yield strength (130 MPa) and its endurance limit (140 MPa). No measurable mass loss was apparent for the 'non-erosive' condition however whereas only a small amount of mass loss could be measured for the 'slightly-erosive' condition. This could be due to a considerable amount of plastic deformation taking place, also apparent in the SEM images, leading to that small observed amount of mass loss. The next two conditions, correspond to higher amounts of mass loss and this is also represented by the obtained stress values which are either comparable or above the ultimate strength (350 MPa) of the material.

In all cases results were highly reproducible and as such an erosion threshold in terms of stress could be established for each one of the materials with regards to ultrasonically induced cavitation. This threshold was in two cases in good agreement with the mechanical properties of the materials (grade DH36 steel, stainless steel), whereas in the case of Cupronickel was above its yield strength and endurance limit. In this case the resulting high stress values were possibly corresponding to a considerable amount of plastic deformation accompanied by zero or minimal mass loss, Nevertheless, they could still be used as indicators of cavitation erosion intensity in a calibrated system.

5.4 Acoustic emission measurements on a reduced–scale rudder model

Following successful application of acoustic measurements on small plates it was decided to extend this research to ship rudders. As such a reduced-scale rudder model was manufactured from steel and was subjected to ultrasonically induced cavitation in a similar way to the small plates.

The reduced-scale rudder model was placed inside a large water tank by means of two elastic bands, in order to isolate it acoustically whereas the ultrasonic transducer–sonotrode was placed just above its top surface. This arrangement can be seen in Figure 7.

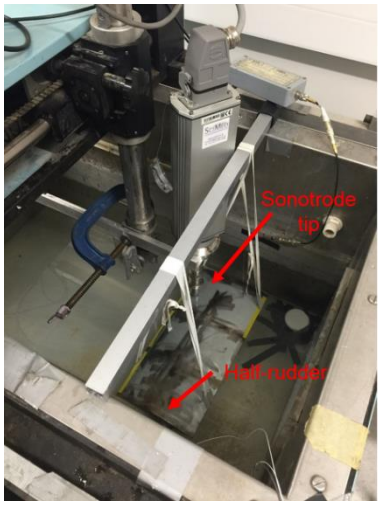

Figure 7: Reduced-scale rudder model positioned inside the water tank. The ultrasonic transducer – sonotrode lies just above its top surface.

Initially, cavitation erosion intensity measurements were conducted using a piezoelectric acoustic sensor. Acoustic emission signals were translated into stresses following a procedure similar to the one described in Section 5.3 and were obtained for different test configurations, leading to cavitation erosion of varying intensity. Moreover, and due to the size of the rudder, the parameter of distance from the sensor was also considered in this case and as such three different sonotrode-placements were examined.

The different sonotrode placements that were examined along with the piezoelectric sensor can be seen in Figure 8.

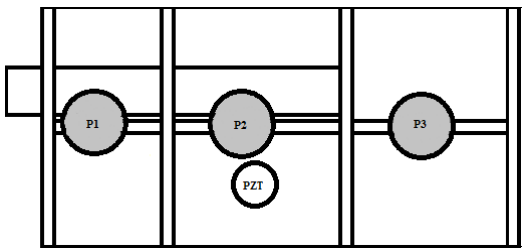

Figure 8: Illustration showing the piezoelectric sensor and the different sonotrode (ultrasonic transducer) placements P1, P2 and P3.

Stress distribution results for various test rig configurations and sonotrode placements can be seen in Figure 9.

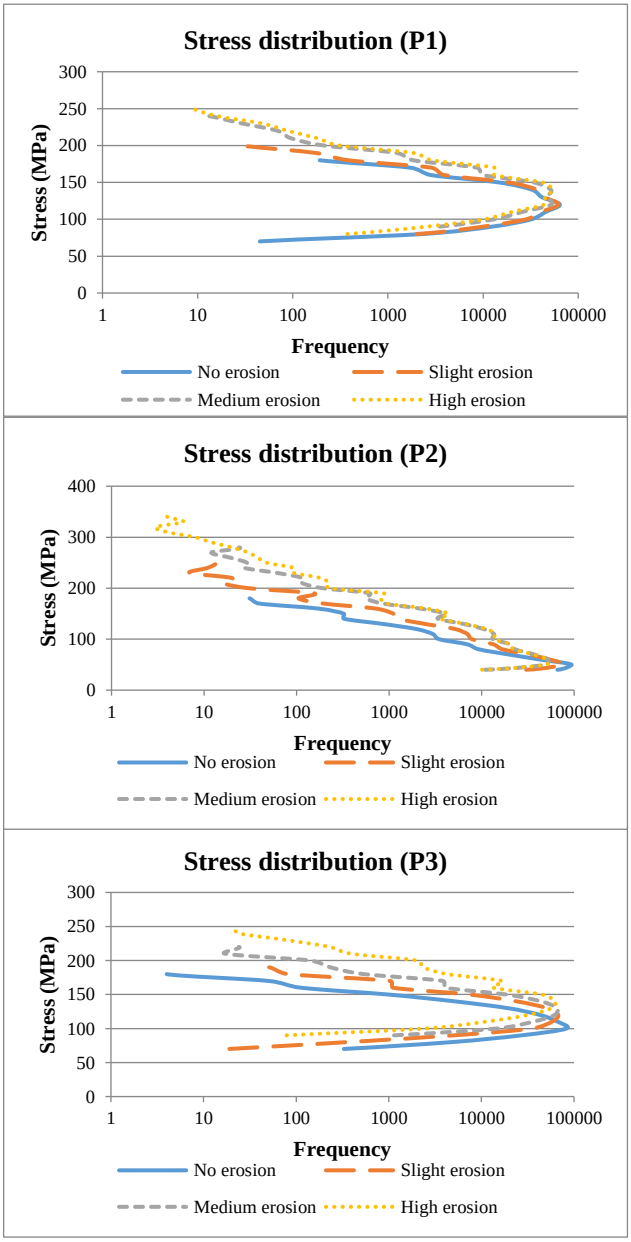

Figure 9: Stress distributions obtained from acoustic emission signals. Top – P1, Middle – P2, Bottom P2.

It can be seen that in relation to the 'non-erosive' condition identical stress values of the order of 180 MPa were obtained for all sonotrode placements. The same applies for the next 'slightly-erosive' condition for which values ranging from 200 to 220 MPa were obtained. It should be noted that, similar to the measurements conducted on a small steel plate, these values are in good agreement with the mechanical properties of the rudder (steel). As for the even higher settings it appears that those signals attenuate with distance whereas when the sonotrode operates just above the acoustic sensor, stress values of the same order with the ones obtained for the small plate are measured.

In addition to cavitation erosion intensity measurements it was decided to explore whether cavitation can be located accurately on the reduced-scale rudder model using an array of acoustic sensors (both piezoelectric and FBGS) or not. Those cavitation source location measurements were

based on the principle of triangulation as it was described by Tobias (1976).

The basis of this technique lies on an array of three acoustic sensors S_0 (0, 0), S_1 (x_1, y_1), S_2 (x_2, y_2) and an acoustic emission source P (x, y) as it can be seen in Figure 10.

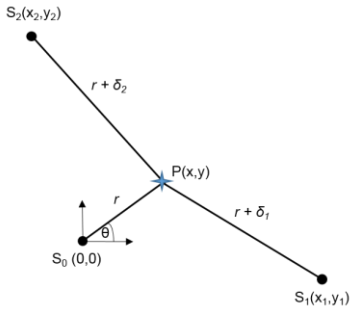

Figure 10: Illustration of the principle of triangulation.

The acoustic emission source P (x, y) would lie at the intersection of the three circles with a radius of r, r +δ_1, r + δ_2 whereas the corresponding centres of those circles would lie at the positions of the relevant sensors. Those circles are described by Equations (3), (4) and (5).

$$x^2 + y^2 = r^2 \quad (3)$$

$$(x - x_1)^2 + (y - y_1)^2 = (r + \delta_1)^2 \quad (4)$$

$$(x - x_2)^2 + (y - y_2)^2 = (r + \delta_2)^2 \quad (5)$$

where δ_1 and δ_2 represent the time delay regarding the arrival of an acoustic emission signal between sensors S_1-S_0 and S_2-S_0 respectively, multiplied by the speed of sound in the examined material.

Under that context, cavitation was induced at different areas on the surface of the rudder, whereas acoustic emission signals from four piezoelectric and FBG sensors were simultaneously captured. Afterwards, time delays between all acoustic sensors were individually calculated while the coordinates of the cavitation source were analytically derived through the aforementioned equations.

A typical time delay between FBG acoustic sensors, positioned at different spots, originating from a cavitation source on the surface of the rudder can be seen in the waveforms presented in Figure 11. Similar waveforms were obtained from piezoelectric sensors.

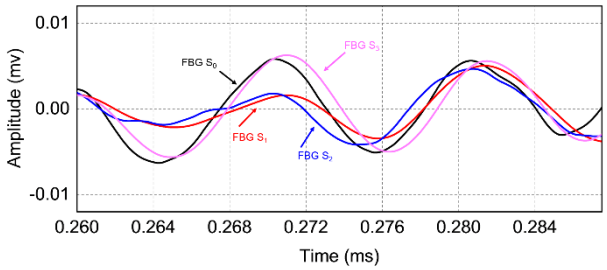

Figure 11: Time delay of waveforms obtained by FBG sensors, position at different spots of the rudder surface.

A total of eleven (11) different sonotrode placements over the surface of the rudder were examined. These can be seen in Figure 12 and Table 1 along with the analytically derived cavitation source coordinates using arrays of both piezoelectric (PZT) and FBG sensors.

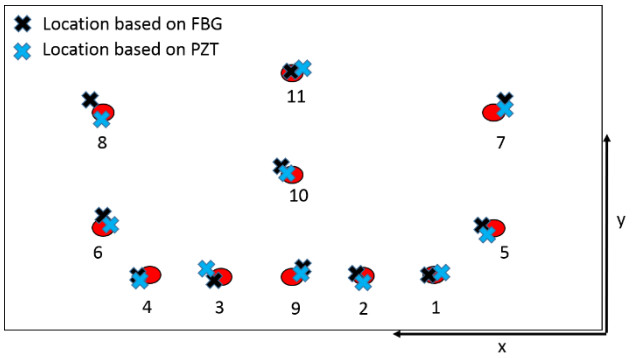

Figure 12: Calculated cavitation source locations using two types of acoustic sensors. Red dots represent the actual location of the sonotrode-cavitation source.

Table 1: Calculated cavitation source locations using two types of acoustic sensors.

Actual coordinates of sonotrode location (cm)	Calculated coordinates from FBGs (cm)	Calculated coordinated from PZTs (cm)
(10, 0)	(11, 0.2)	(9.4, 0.28)
(13, 0)	(13.4, 0.24)	(13, 0.12)
(16, 0)	(15.2, 0.4)	(15.3, 0.25)
(19, 0)	(19.7, 0.1)	(20.8, 0.35)
(22, 0)	(23.1, 0.25)	(23, 0.24)
(8, 3.2)	(9.2, 3.4)	(9, 3.1)
(24, 3.2)	(24.2, 3.6)	(23.8, 3.4)
(8, 9.8)	(7.4, 10.4)	(7.4, 10.1)
(24, 9.8)	(26.4, 10.5)	(24.1, 9.6)
(16, 7.5)	(16.8, 7.6)	(16.2,7)
(16, 13)	(16.2, 14)	(15.9, 13)

It appears that both piezoelectric (PZT) and fibre Bragg gratings (FBG) are capable of locating cavitation all over the rudder surface. Slight discrepancies that are observed, are believed to be caused, primary due to minor reflections of acoustic signals related to the shaft and stringers inside the rudder and secondly due to signal filtering.

6 CONCLUSIONS

The effects of ultrasonically induced cavitation erosion on common shipbuilding materials were examined both in quantitative and qualitative terms. Good correlation between mass loss measurements and fractographic observations was achieved. A methodology through which acoustic emissions related to ultrasonically induced cavitation could be translated into stresses was also successfully developed. Results were in good agreement with other measurements and observations as well as the mechanical properties of the examined materials. In addition, acoustic-stress thresholds relating to erosion were established for each one of the studied materials.

The method was then successfully applied on a reduced-scale rudder model, for cavitation erosion intensity-stress measurements. A cavitation source location method based on the principle of triangulation, was also effectively developed. Tests were conducted using both an array of piezoelectric and fibre Bragg grating acoustic sensors. Results indicate that acoustic emissions can potentially be used as means of cavitation erosion monitoring, both in terms of location and intensity, in ship rudders.

REFERENCES

Bark, G., Berchiche, N. & Grekula, M. (2004). 'Application of principles for observation and analysis of eroding cavitation'. EROCAV observation handbook. Ed. 3.1. Chalmers University of Technology, Sweden.

Besant, W. (1859). Hydrostatics and Hydrodynamics. Cambridge University Press.

Carlton, J. (2012). Marine propellers and Propulsion. Ed. 3. Butterworth-Heinemann.

Carpinteri, A, Lacidogna, G. & Pugno, G. (2007). 'Structural damage diagnosis and life-time assessment by acoustic emission monitoring'. Engineering Fracture Mechanics **74**, pp. 273-289.

Dunegan, H. (1969). 'Ultrasonic acoustic emissions from materials'. IEEE Transactions of Sonics and Ultrasonics **16**(1), pp. 32-35.

Euler, M. (1756). 'Théorie plus complete des machines qui sont mises en movement par la reaction de l'eau'. L'Académie Royale des Sciénces et Bélles Léttres, Berlin.

Fortes-Patella, R., Reboud, J. L. & Briancon-Marjollet, L. (2004). 'A phenomenological and numerical model for scaling the flow aggressiveness in cavitation erosion'. Cavitation Erosion Workshop, Val de Rueil, France.

Franc, J.P. & Michel, J.M. (2004). Fundamentals of cavitation. Springer Netherlands.

Gautschi, G. (2002). Piezoelectric sensorics: Force Strain Pressure Acceleration and Acoustic Emission Sensors Materials and Amplifiers. Sringer Berlin Heidelberg.

Giurgiutiu, V. (2003). 'Lamb wave generation with piezoelectric wafer active sensors for structural health monitoring'. Proceedings of SPIE 5056, pp. 111-122.

Grattan, K.T.V. & Sun, T. (2000). 'Fiber optic sensor technology: An overview'. Sens. Actuators A:Phys **82**, pp. 40-61.

Kaiser, J. (1953). 'Experimental Observations and Theoretical Interpretations of Sound Measurement During Tensile Loading of Metals'. Archiv fur das Eisenhuttenwesen **24(**1/2), pp. 43-45.

Karimi, A. & Martin, J.L. (1986). 'Cavitation erosion of materials'. International Metals Reviews **31**, pp. 1-26.

Lindau, O. & Lauterborn, W. (2003). 'Cinematographic observation of the collapse and rebound of a laser-produced cavitation bubble near a wall'. Journal of Fluid Mechanics **419**, pp. 327-348.

Mal, A.K., Ricci, F., Gibson, S. & Banerjee, S. (2003). 'Damage detection in structures from vibration and wave propagation data'. Proceedings of SPIE 5047, pp. 202-210.

Mihailov, S.J. (2012). 'Fiber Bragg grating sensors for harsh environments'. Sensors 2012 **12**, pp. 1898-1918.

Othonos, A. & Kalli, K. (1999). Fiber Bragg Gratings. Artech House Inc.

Parsons, C. & Cook, S. (1919). Trans. Inst. Nav. Arch. **61**, pp. 233-240.

Philip, A. & Lauterborn, W. (1998). 'Cavitation erosion by single laser-produced bubbles'. Journal of Fluid Mechanics **361**, pp. 75-116.

Pollock, A.A. (1968). 'Stress-Wave Emission – A New Tool for Industry'. Ultrasonic **6**, pp. 88-92.

Portevin, A. & Le Chatelier, F. (1923). Compte. Rendu **176**, pp. 507-510.

Rayleigh, L. (1917). 'The pressure developed in a liquid during the collapse of a spherical cavity'. Phil. Mag. **34**.

Reynolds, O. (1873). 'The causes of the racing of the engines of screw steamers investigated theoretically and by experiments'. Trans. INA.

Rogers, L.M. (2001). Structural and Engineering Monitoring by Acoustic Emission Methods – Fundamentals and Applications. Lloyd's Register, Technical Investigation Department.

Schofield, B.H. (1958). Acoustic Emission Under Applied Stress. U.S.A.F., Wright Air Development Centre, WADC-TR-58-194, NTIS Accession No. AD 155674.

Tan, A.C.C., Kaphle, M. & Thambiratnam, D. (2009). 'Structural Health Monitoring of Bridges Using Acoustic Emission Technology'. Proceedings of the 8th International Conference on the Reliability, Maintainability and Safety, Chengdu, China.

Tobias, A. (1976). 'Acoustic emission source location in two dimensions by an array of three sensors'. Nondestructive Testing **9**, pp. 9-12.

Votava, E. & Jax, P. (1979). Inspection of Nuclear Reactors by Means of Acoustic Emission During Hydro-test. Kraftwerk Union A.G., Erlangen, Germany.